*Design of Machines and Structures, Vol. 2, No. 1 (2012), pp. 35–51.*
*https://doi.org/10.32972/dms.2012.004*

# RESULTS OF LABOARATORY TESTS OF HARMONIC GEAR DRIVE

JÓZSEF PÉTER–GÉZA NÉMETH
Department of Machine and Product Design
3515 Miskolc-Egyetemváros
machpj@uni-miskolc.hu; machng@uni-miskolc.hu

**Abstract**
The constraint of the reliable operation of a gear drive is the proper stiffness of the structural elements, so the stiffness of the gears. One of the variant of the planetary gear drives is the harmonic gear drive, which essence is the flexibility of one or both elements of the gear pair. The flexible gear body changes its shape due to the structure of wave generator and gear pair, and also due to the external loads of the drive. The mesh of the gears is the function of the degree and nature of deformation. This paper is dealing with the laboratory test of a drive produced for experimental purposes.

## 1. Introduction

Since the foundation of the Department of Machine and Product Design (formerly the Department of Machine Elements) at the University of Miskolc there has been research works in relations with planetary gear drives. One of the variant of the drive is the harmonic gear drive that has been belonging to the area of examined drives since the middle of 1970s. One of the constraints of the design and production of the harmonic gear drive (hereinafter referred to as harmonic drive) is the knowledge of the meshing and the interaction of the rigid and flexible gear pair. In paper [2] the author dealt with the theory and laboratory test of the meshing of harmonic drive, in paper [3] the analysis was expanded by the study of the waving gear coupling and the calculations of the deflection of flexible gear due to loads. In the paper the authors summarize all the knowledge necessary to the interpretation of the laboratory test results and the newer results of the analysis of test results.

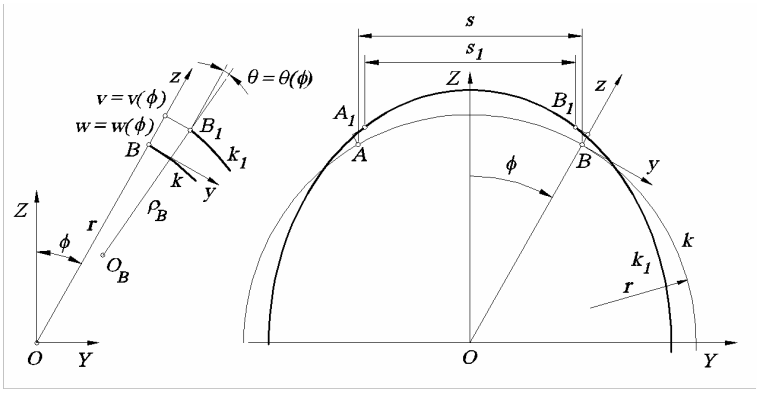
## 2. Elastic deflection of bodies

Although the relation between load and the elastic deformation of bodies due to load has been widely known there are relatively few mechanisms the operation of which is based on this recognition. The majority of mechanisms is based on the rigid body model to the present day. Clerence Walton Musser was the inventor who summarized in paper [1] the principles that can be the basis of the operation of mechanisms, starting from Robert Hooke's well known formula which states that the elastic deflections of bodies are proportional to the loads. These principles are the arcuation, the integration, the scalloping, the differentiation, the interfacial strain, the Poisson's wedge, the torsion lever and the twisted strip. In [5] the authors dealt with the arcuation, the integration and the scalloping in detail, keeping the harmonic drive and the waving gear coupling in mind.

## 3. The arcuation

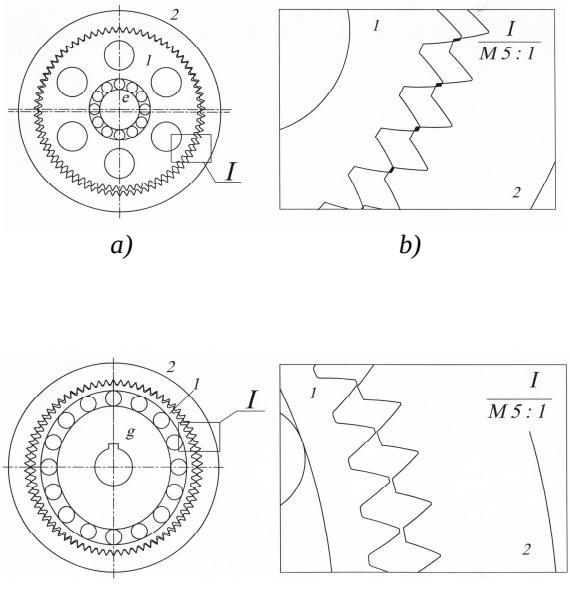
At *Figure 1*. the neutral line, k of a prismatic flat curved beam is visible which is transformed to k' curve, due to load. The neutral line, k is an arc with radius, r. The tangential

displacement of one of its arbitrary point having φ coordinate is $w = w(\phi)$ and its curvature is $\kappa(\phi) = \frac{1}{\rho(\phi)} = -\frac{1}{r^2}\left(\frac{d^2 w}{d\phi^2} + w\right)$. By increasing the curvature of the beam the chord length, AB is decreasing. The increment of the chord length is the function of curvature, i.e. $s_1 - s = f(\rho(\phi) - r)$.




a) b)

*Figure 1. Arcuation. a) The displacement of an arbitrary point and b) the change in chord length*




a) b)

c) d)

*Figure 2. a) and b) Planetary gear drive, c) and d) Harmonic gear drive*

In *Figure 2. a)* a planetary gear drive having an internal connection gear pair *1* and *2* and an eccentric, *e* connecting them is visible. In *Figure 2. c)* a harmonic gear drive consisting of an internal connection gear pair *1* and *2* and a wave generator, *g* deflecting the external toothed gear to elliptic shape is visible. The gears *1* and *2* and the eccentric, *e* of the planetary gear drive is regarded as rigid. The circular spline, 2 and the wave generator, g of the harmonic drive is also rigid. The external toothed gear (flexspline), *1* of the harmonic drive is deflected elastically due to the wave generator, *g*.

The angular velocities of the elements of planetary drive relatively to the housing are $\omega_1$, $\omega_2$ and $\omega_e$, that of the gear pair relatively to the eccentric are $\omega_{1e} = \omega_1 - \omega_e$ and $\omega_{2g} = \omega_2 - \omega_g$ . The ratio of angular velocities $\omega_{1e}$ and $\omega_{2e}$ is defined by the ratio of number of teeth, $z_1$ and $z_2$, i.e. $u = \frac{z_2}{z_1}$. If gear $1$ drives gear $2$, ($1 \to 2$), the ratio of angular velocities relatively to the eccentric, $e$ is $i_{12} = \frac{\omega_1 - \omega_e}{\omega_2 - \omega_e} = u$. In case of $\omega_2 = 0$ and $e \to 1$ the ratio is $i_{e1} = \frac{\omega_e}{\omega_1} = \frac{1}{1-u}$. To increase the ratio, the number of teeth, $z_1$ should be increased and/or the difference of tooth numbers, $z_2 - z_1$ should be decreased. The increment of tooth numbers increases the radial dimensions and the decrement of the difference of tooth numbers causes interference between root and crest as *Figure 2. b)* shows.

The external toothed gear, *1* of the harmonic drive is deflected to elliptic shape by the wave generator, g and the curvature along its circumference is changing similarly to the beam shown in *Figure 1. b).* The teeth of the flexible spline, $1$ can mesh the teeth of circular spline, $2$ in the stage having greater curvature. At this stage the chord lengths among the tooth tip edges of the flexible spline are decreased and **there is no interference between the teeth** of the gears, as shown in *Figure 2. d).* The tooth number difference is integral multiple of the wave number, for symmetry. When the wave number, $N = 2$, the minimum of the tooth number difference, $z_2 - z_1 = 2$.

**4. Harmonic gear drive or gear drive service**

The planetary drive shown in *Figure 2. a)* can be studied **in both gear drive and planetary gear drive service**. In gear drive service the frame of reference is fixed to the eccentric, $e$ and the interaction of the gears turned relatively to the eccentric is analysed. In planetary gear drive the frame of reference is fixed, e.g. to the circular spline, *2* and the interaction of external gear, 1 and internal gear 2 is studied in the slewing of the eccentric.

On the analogy of planetary drive the harmonic drive can be analysed **in gear drive or harmonic gear drive service**. First case, the swivel of pair of gears is analysed in the frame of reference fixed to the wave generator, in harmonic gear drive service the weaving motion of the external gear is examined in the frame of reference fixed to the circular spline. As the investigation of gear pair meshing, the occurrence of interference disturbing the meshing and the interaction of the elements of the drive are more clear in gear drive

service, **the following analyses are made in the frame of reference fixed to the wave generator**.

**5. Reducing and multiplying drive**

The gear drive speeds down when the ratio, $i = \frac{\omega_{driving}}{\omega_{driven}}$ is $i < -1$, or $i > +1$, and seeds up when $-1 < i < 1$. The harmonic gear drive speeds down when the wave generator, *g* is the driving element and the gear *1* or *2* is driven besides the fixed *2* or *1* gear to the frame. In this case the driving direction is $g \to 1$ or $g \to 2$. The harmonic gear drive speeds up when the direction of drive is $1 \to g$, or $2 \to g$. The relations are summarized in *Table 1*.

*Table 1.*

| | | | | | | | |
|---|---|---|---|---|---|---|---|
| *Speeds down* | *Gear drive* | $1 \to 2$ | $i_{12} = u$ | *Speeds up* | *Gear drive* | $2 \to 1$ | $i_{21} = \frac{1}{u}$ |
| | *Harmonic gear drive* | $g \to 1$ | $i_{g1} = \frac{1}{1-u}$ | | *Harmonic gear drive* | $1 \to g$ | $i_{1g} = 1-u$ |
| | | $g \to 2$ | $i_{g2} = \frac{1}{1-\frac{1}{u}}$ | | | $2 \to g$ | $i_{2g} = 1-\frac{1}{u}$ |

**The comparison of mechanical powers gives the feasibility of decision** if which sence of power flow of the gear drive $1 \to 2$ or $2 \to 1$ is the equivalent of the sence of power flow in harmonic gear drive service. The basis of analysis is the equilibrium of the drive and the assumption stating that the magnitude and sense of torques $M_g, M_1$ and $M_2$ are acting to the elements of *g*, *1* and *2*, respectively, are not dependent on the frame of reference.

In the frame of reference fixed to the housing the mechanical power flowing through the gears *1* and *2* are $P_1 = M_1 \omega_1$ and $P_2 = M_2 \omega_2$, respectively, and that of the powers in the frame of reference fixed to the wave generator $P_{1g} = M_1(\omega_1 - \omega_g)$ és $P_{2g} = M_2(\omega_2 - \omega_g)$. On the basis of *Table 2.* the sign of power ratios and their consequences are studiable. In case *(1)* the ratio of powers $P_{1g}$ flowing on the gear *1* with $\omega_{1g} = \omega_1 - \omega_g$ angular velocity relative to the wave generator and $P_1$ flowing on the gear *1* with $\omega_1$ angular velocity relative to the frame is positive so in the services of both gear drive and harmonic gear drive the gear 1 is the driving or the driven element. The senses of power flow are $1 \to 2$ and $1 \to g$, or $2 \to 1$ and $g \to 1$.

In case *(2)* the ratio of powers $P_{2g}$ flowing on the gear *2* with $\omega_{2g} = \omega_2 - \omega_g$ angular velocity relative to the wave generator and $P_2$ flowing on the gear *2* with $\omega_2$ angular veloc-

ity relative to the frame is negative. In this case the power flow $1 \to 2$ suits $2 \to g$ , and that of $2 \to 1$ suits $g \to 2$ .

*Table 2.*

| *Power ratio* | | *Power flow* | |
|---|---|---|---|
| | | *Harmonic gear drive* | *Gear drive* |
| *(1)* | $\frac{P_{1g}}{P_1} = \frac{M_1(\omega_1 - \omega_g)}{M_1\omega_1} = \frac{u}{u-1} > 0$ | $1 \to g$ | $1 \to 2$ |
| | | $g \to 1$ | $2 \to 1$ |
| *(2)* | $\frac{P_{2g}}{P_2} = \frac{M_2(\omega_2 - \omega_g)}{M_2\omega_2} = \frac{1}{1-u} < 0$ | $2 \to g$ | $1 \to 2$ |
| | | $g \to 2$ | $2 \to 1$ |

## 6. The meshing of harmonic gear drive

The paper [4] deals in detail with both the mechanical model used to the analysis of meshing of harmonic gear drive and the occurrence of interference disturbing the meshing.

### *6.1. Tooth profile*

Te applied tooth profile is an involute curve, the base profile angle, $\alpha = 20^o$ , the addendum factor, $h_a^* = 1$, the radial clearance factor, $c^* = 0,25$. In the course of tests **the flexible gear was manufactured as a cylindrical gear by hobbing and the internal gear was generated by pinion cutter**.

### *6.2. Flexible gear, flexspline*

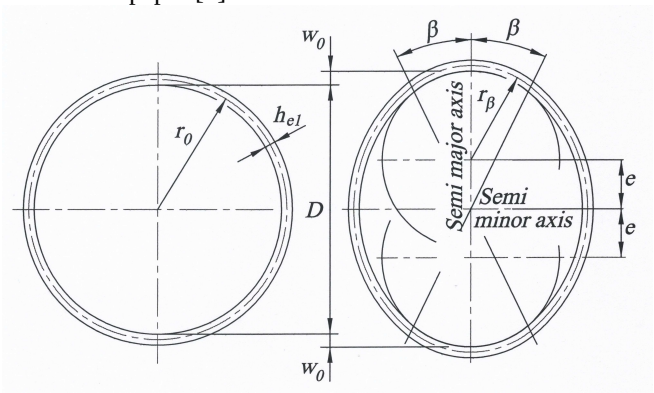
The flexible gears are cup shaped. The profile correction factors, $x_1$ of the flexible gears, *H21* and *H22* were chosen larger than it was recommended (in the range of number of teeth, $z_1 = 100...800$ $x_1 = 3...4$ ). The *Table 2.* in paper [7] contains the profile correction factors both as intended, ( $x_1$ ) and as determined by measurement over pins, ( $x_{1m}$ ). The recommended height of the tooth of flexible gear, $h_1 = 1,4...1,6\ m$ In case of the *gear, H21* this tooth height is less than the offered one and in case of the *gear, H22* it is bigger. The relation between the tooth height and the number of teeth meshing at one time are examined by the tooth height deviated from the recommended value. The offered value of the face width of flexible spline, $b_1 = 0,2...0,4D$ . The face width was chosen less than offered to avoid the interference appeared at the back part of the tooth tip.

In the course of dimensioning and strength calculations the flexible gear was substituted by a hollow cylinder having a wall thickness, $h_{e1}$ and length, $L_{e1}$ to simplify the problem. The neutral surface of the hollow cylinder is a straight cylinder with radius, $r_0 = \frac{D + h_{e1}}{4}$. The wall thickness underneath the teeth, $h_0 = \frac{d_{f1} - D}{2}$, the equivalent thickness considering the effect of the teeth due to flexural rigidity, $h_{e1} = h_0 + m$, where $m$

is the module. The length of the hollow cylinder, $L_{e1} = b_1 + \frac{L_1 - b_1}{3}$ comprises also the superficies following the teeth and having the role of a compensating coupling where $b_1$ is the tooth width of the flexible gear.

*6.3. The circular spline*

The flexible spline and circular spline are meshing in the vicinity of the semi major axis, prior to the appearance of the external loads, as shown in *Figure 3.* **Along the semi major axis of the wave generator the centre distance,** $O_1O_2 = a_w$ **is equal to the radial deflection of the flexible spline**, $a_w = w_0$ . When the profile correction factor of the circular spline along the major axis is calculated by the constraints of backlash-free mesh, $x_2 = \frac{z_2 - z_1}{2} \frac{inv\alpha_{wt} - inv\alpha}{tan\,\alpha} + x_1$ is obtained, where the pressure angle, $\alpha_{wt} = arc\,cos \frac{z_2 - z_1}{2} \frac{m}{w_0}$. The revealing dimensions of circular splines, *G22* and *G23* are collected in *Table 4*. of paper [7].




*a)* *b)*

*Figure 3. a) Ring substituting the flexspline b) Ring deflected by two disks with eccentric bearing support*

*6.4. Wave generator*

The elliptically deformed fleible spline and the rigid circular spline are brought in connection by the wave generator. Two wave eccentric disk wave generator (and elliptical cam wave generator, not discussed in present paper) were used. The two wave eccentric disk wave generator consists of two eccentric, two disks and commercially available rolling bearings.

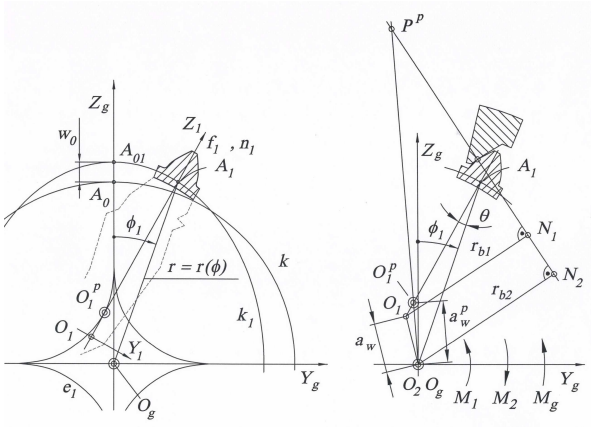
a) In the course of research the ratio of radial deflection/module, $w_0/m$ wa changed to the values of $0.6, 0.7, 0.8, 1.1, 1.2, 1.3$ by altering the flexible spline, the eccentric and the disks due to *Table 3.* [7]. **By changing the element of the drive the relation between the radial displacement, $w_0$ the semi arc of contact between the flexspline and wave generator disks, $\beta$, shown in *Figure 3.* and the deflection of flexspline, described by the radius of curvature, $\rho$ were inspected.**

b) The flexible spline is influenced by the disk which has bearing support with eccentric, $e$, and diameter, $d_t$, along an arc of central angle, $2\beta$. The suggested range of $\beta$, considering the magnitude of the bending stress in the vicinity of the semi major and semi minor axes is $\beta = 20^o ... 40^o$. Along the arc of contact the radius of curvature of the neutral line, $r_\beta = r_0 + w_0 - e$ is constant, the radius of disk is $r_t = r_\beta - \frac{h_{e1}}{2}$. The relation between the data of $w_0$, $r_0$, $r_\beta$ and $\beta$ can be expressed by the formula

$$\frac{(r_0 - r_\beta) r_0}{w_0 r_\beta} = \frac{\frac{4}{\pi}(\cos\beta + \beta\sin\beta) - 2\sin\beta}{\frac{\pi}{2} - \sin\beta\cos\beta - \beta - \frac{4}{\pi}(\cos\beta + \beta\sin\beta) + 2\sin\beta}.$$

The values of $\beta$ computed by given $w_0$, $r_0$ and $r_\beta$ data are collected in *Table 3.* [7].

*6.5.The mesh of the elastic external teeth gear (flexsline) and the rigid internal teeth gear (circular spline)*



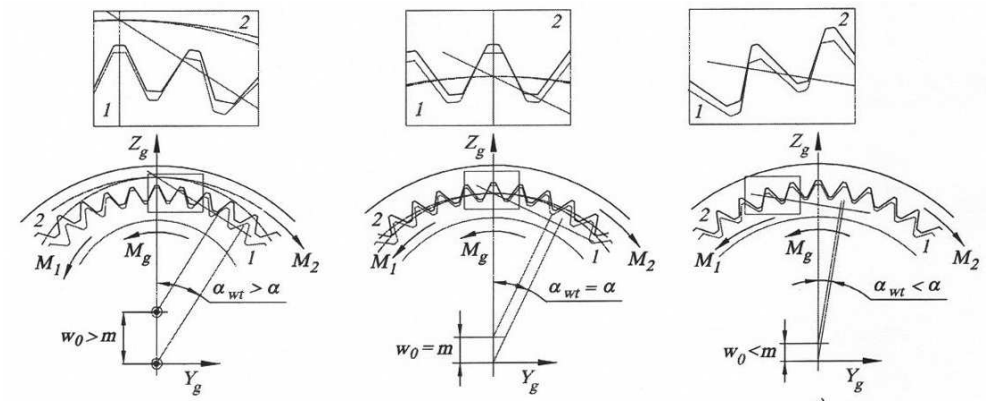

*a)* *b*

*Figure 4. a) Deflected flexspline, b) Profile mesh, c) Edge mesh*

The deflected elastic gear (flexspline) is shown in *Figure 4. a).* There are some assumptions around the tooth. Its axis of symmetry, $f_1$ is the normal of neutral line, $k_1$. The

centre of base circle, $O_1$ belonging to the involute tooth profiles is situated along the axis of symmetry, $f_1$. The momentary centre of rotation of the tooth during the traverse of flexspline in relation to the wave generator is $O_1^p$.

The engage of one pair of tooth of the flexible-rigid pair of gears can be studied in *Figure 4. b).* It can be traced back to the engage of an external teeth gear with geometric centre, $O_1$ and a shifted centre of rotation $O_1^p$, and an internal teeth gear with coincident geometric centre and centre of rotation, $O_2$.




*a)* *b)* *c)*

*Figure 5. The location of meshing teeth in relation to the semi major axis of the wave generator as the function of radial deflection,* $w_0$

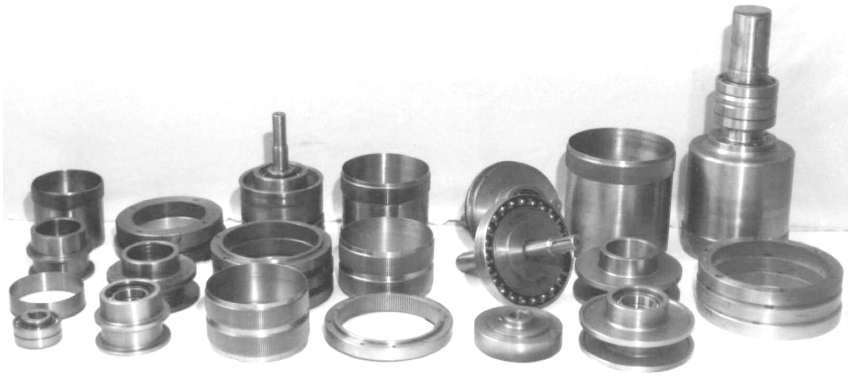
**The location of meshing teeth in relation to the semi major axis of the wave generator is changing in the function of radial deflection,** $w_0$, as shown in *Figure 5.* The suggested range of $w_0$ is $1{,}1...1{,}2\ m$, which is reduced due to the elastic deflection of the elements and the rearranging of clearances.

In front of and behind the profile mesh the gap in direction of the normal between the tooth profile and the tooth tip edge, is so small in a relatively wide range, that the elastic deflection of **the elements are meshing edge-like way too**. The basis of the investigation of the edge mesh is **the knowledge of the gap in normal direction and the elastic deflection due to loading of the drive elements**. The papers [2, 3] deal in detail with the components of elastic deflection of harmonic gear drive and the edge mesh.

### 7. The typical data of the elements of test drive

The typical size of the harmonic gear drive is the nominal (N) inner diameter $(ND)$, which is approximately identical with the actual inner diameter $(D)$ of the flexible gear drive. The elements of harmonic drive with the nominal diameter of *ND* 120, 160 and 190

are shown in *Figure 6*. These elements were manufactured in the laboratory of Department of Machine Elements, University of Miskolc, and the tests were made on the elements having the nominal diameter *ND190* . The geometry data of drive element were summarized in paper [7], *Table 2., 3.* and *4.*



*a)* *b)* *c)*

*Figure 6. Basic elements of the Harmonic drive.*
*a) ND120 , b) ND160 , c) ND190 drive elements*

*7.1. The test place building up*

The drive box shown in *Figure 7.* was fixed on a machine base and the circular spline, $2$ was fixed to the drive box $(\omega_2 = 0)$. The wave generator, $g$ was revolved in relation to the drive box through a torque measuring shaft. The torque $M_1$ acting to the flexspline, $1$ was changed by the loading disks, $6$ . With regard to the end face of the drive the $M_1$ acts counter clockwise as shown *in Figure 8.* and *9.* The wave generator was revolved counter clockwise in slow down service $(g \rightarrow 1)$ and clockwise in speed up service $(1 \rightarrow g)$ .

*7.2. Recording the test data*

The radial displacement of flexspline, the change of its radius of curvature and the load acting to the tooth of flexspline was recorded according to *Figure 8.*, as the function of deviation, $\varphi_g$ in relation to the circular spline.

*7.3. Measurement of the radial displacement*

The radial displacement of the fexspline, $w$ was measured next to the tooth, in a plane parallel to the end face of the flexspline. The measuring gauge that consist of feather and feeler, wes fixed to the circular spline. The displacement was recorded by strain gauges glued to the two sides of the feather, in the function of the wave generator deviation relatively to the circular spline. The dicplacement of $w = 0$ was recorded previously to putting

the wave generator into the flexspline. The unit of displacement was determined at the tip of deformational wave, $(\phi_g = 0)$ on the basis of generator geometry $\left( w_0 = e + \frac{d_t}{2} - \frac{D}{2} \right)$.

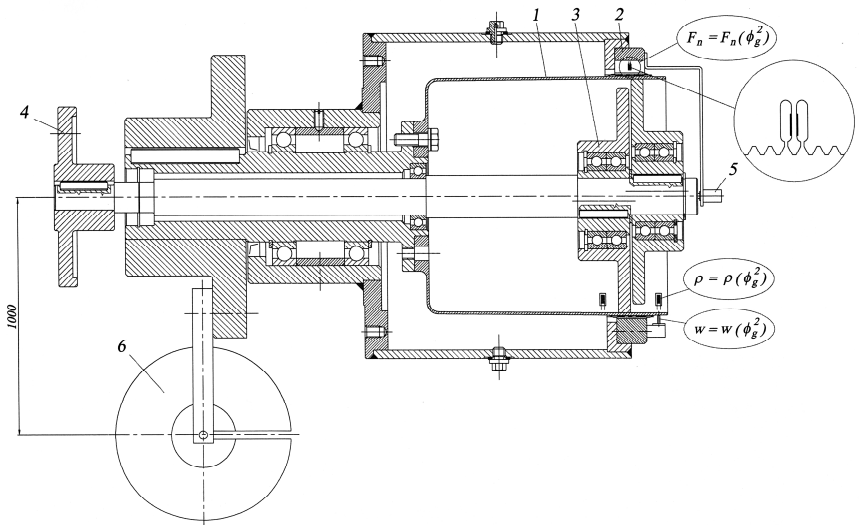
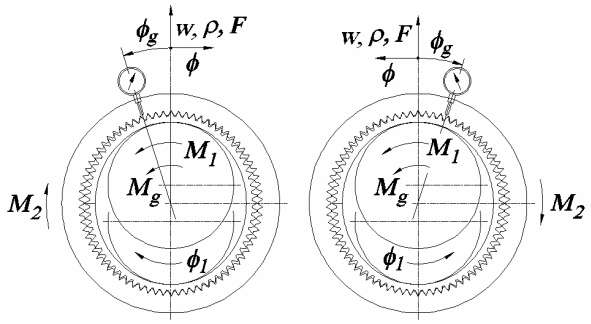
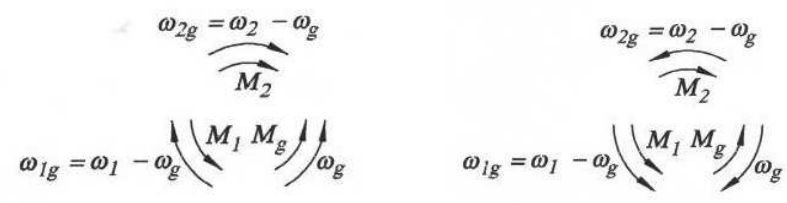



*Figure 7. Experimental drive. 1 flexspline, 2 circular spline, 3 wave generator, 4 coupling, 5 rotating transducer, 6 loading disk*




*a)* *b)*

*Figure 8. The wave generator deviation and the recording of measured amounts in harmonic gear drive service. a) The harmonic drive slows down, b) speeds up*




*a)* *b)*

*Figure 9. Torques acting to the elements of the drive and the angular velocities in gear drive service.*
*a) The gear drive slows down, b) speeds up*

*7.4. Measuring the radius of curvature*

During the tests the tangential elongation of the cenre layer of the flexspline is supposed to be negligibly small ($(\varepsilon_{\phi 0} \approx 0)$). In normal direction, at $\frac{h_0}{2}$ distance from the centre surface of flexspline, parallelly to the end surface of flexspline, the strain $\varepsilon_\phi = \varepsilon_\phi(\phi_g)$ originated from the bending is measurable by strain gauges. Knowing the strain the radius of curvature is $\rho = \frac{1}{\frac{1}{r_0} + \varepsilon_\varphi(\varphi_g)\frac{h_0}{2}}$.

The change of the radius of curvature is measured in a plane, parallel with the end surface of the flexspline, next to the teeth. The strain gauges are glued next to the teeth. The strain complied with the radius of curvature, $r_0$ is allocated prior to putting the generator into the flexspline ($\varepsilon_\phi = 0$). The change of unit of radius of curvature is determined by a measurement at the tip of wave, ($\phi_g = 0$, $\rho_\beta = r_\beta$, in paper [7] *Table 3.* with a generator disk havingknown radius. The radius of curvature is recorded during the deviation of generator relatively to the circular spline.

*7.5. Measuring the force acting to the tooth of circular spline*

To determine the load acting to the tooth of tha circular spline, a measuringh tooth was shaped on the circular spline, on a way shown in *Figure 7*. The measuring tooth is supported by a slender feather, gluing strain gauges on both the sides. The load acting to theteeth is recorded in the function of generator deviation relatively to the circular spline. The load acting to the teeth is determined knowing the load distribution, the number of meshing teeth and the torque acting to the flexspline, $M_1$.

## 8. The measured amounts and the conclusions

The measured amounts in gear drive service are shown in *Figure 10–13*. The power flow of $2 \to 1$ belongs the left hand side and that of $1 \to 2$ belongs the right hand side column. In the case of the power flow $2 \to 1$ the wheels are revolving clockwise relatively to the generator, the teeth of flexspline enter into the spaces of the circular spline on the arc belongs to the angle range of $-\frac{\pi}{4} \le \phi \le 0$ and come out on the arc belongs to the angle range of $0 \le \phi \le \frac{\pi}{2}$. In the case of the power flow $1 \to 2$ the wheels are revolving counter clockwise, the teeth of flexspline enter into the spaces of the circular spline on the arc belongs to the angle range of $0 \le \phi \le \frac{\pi}{2}$ and come out along the section $-\frac{\pi}{4} \le \phi \le 0$.

The number of teeth of the gears and the inner diameter of the flexspline in the inpected cases are $z_1 = 190$, $z_2 = 192$, and $D = 191{,}7\ mm$, respectively. In the cases shown in *Figure 10. a) and c)* the torques acting clockwise to the flexspline are $M_1 = 0\ Nm, 200\ Nm, 400\ Nm, 600\ Nm$, and that of *Figure b)* $M_1 = 0 Nm, 200\ Nm, 400\ Nm$ *és 600 Nm.* In *Figure d)* $M_1 = 0\ Nm, 200\ Nm, 400\ Nm$, and *Figure e)* and *f)* the torque is $M_1 = 600\ Nm$.

In the function of angle $\phi$, measured from the major axis of the generator, the radial displacement, $w$, measured next to the teeth of flexspline is shown in *Figure10. a)* and *b).* The radius of curvature, $\rho$, inspected also next to the teeth of flexspline is shown in *Figure 10. c)* and *d).* In *Figure 10. d)* and *e)* the force acting to the tooth of circular spline is shown.

a) *Figure 10. a) and b)* show the radial displacement of the flexspline. **Applying the load on the drive the flexspline is deflected and the gaps are rearranged and as a consequence, the radial displacement of the flexspline decreases.**
b) *Figure 10. c)* and *d)* show the alteration of the radius of curvature. In case of $M_1 = 0 Nm$ the flexible spline is fitted to the disk along the arc belongs to $2\beta$ as shown in *Figure 3*. **The measured value of the radius of curvature is approximately constant.**
c) In the case of $M_1 > 0,\ 2 \to 1\ and\ 1 \to 2$ the alteration of the radius of curvature is different. **In the case of $2 \to 1$ the disk acts in two stage to the flexible spline. Between these two stages the flexspline is bent and become detached from the disk.**
d) In the case of $M_1 > 0$ and $1 \to 2$ **three special stages can be observed** on the wave. The generator supports the flexspline only on the left hand side of the wave, at the stage of penetration of the teeth of flexspline into the spaces of circular spline. At the tip of wave the flexspline separates from the disk and the circular spline will cause the radius of curvature of the flexspline to be decreased. Emerging from the engagement the radius of curvature of the flexspline is increasing. This stage is followed by another one which has an approximately constant radius of curvature.

*Gear drive service* $2 \to 1$ *Gear drive service* $1 \to 2$

$x_1 = 4{,}555$ , $x_2 = 4{,}958$ , $w_0 = 1{,}2\,mm$ , $e = 3{,}9\,mm$ , $d_t = 186{,}3\,mm$ $\beta = 34{,}757^{o}$

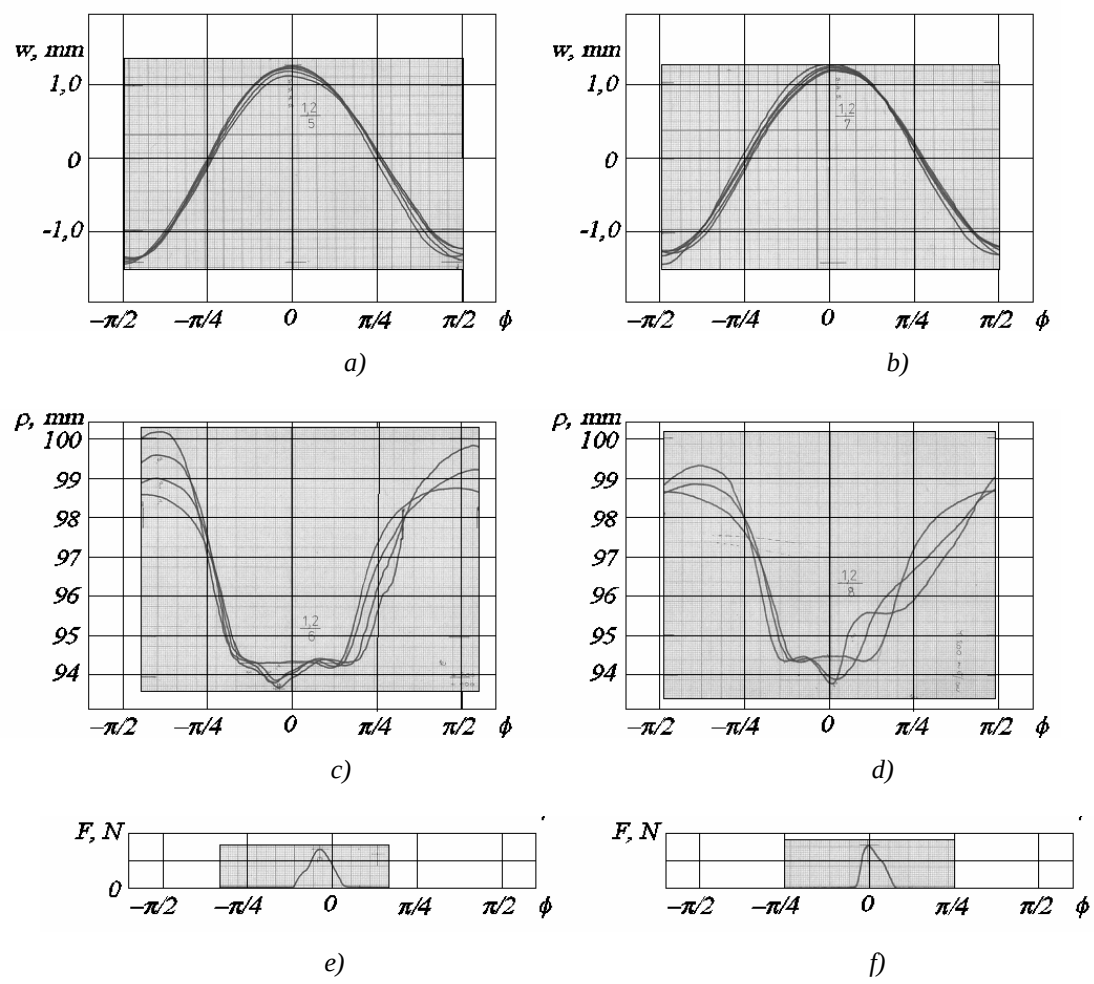
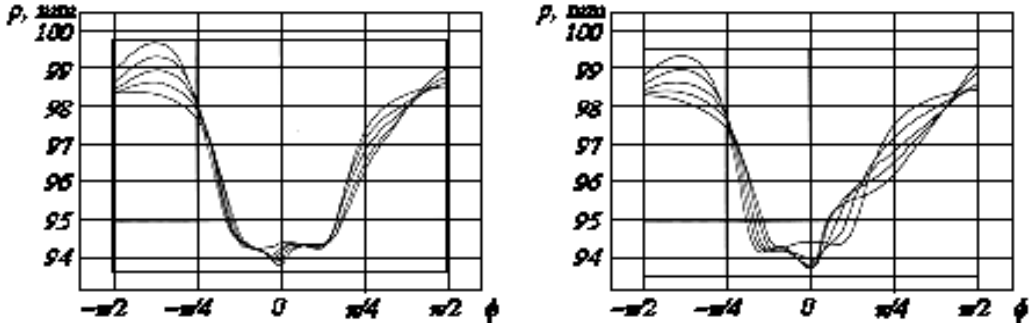



*Figure 10. a) and b) Radial displacement of the flexspline,*
*b) and d)* $\rho$ *is the radius of curvature, e) and*
*f)* $F$ *is the force acting to the tooth of the circular spline*

*Gear drive service,* $2 \to 1$ *Gear drive service,* $1 \to 2$

$x_1 = 4{,}555$ , $x_2 = 4{,}958$ , $w_0 = 1{,}1\,mm$ , $e = 3{,}9\,mm$ , $d_t = 186{,}1\,mm$ , $\beta = 24{,}811^o$




*a)* *b)*

*Figure 11. The radius of curvature, in the function of deviation relatively to the major axis*

e) *Figure 10. e)* and *f)* show the forse acting to the teeth of circular spline in case of the torque value of $M_1 = 600\ Nm$ . **In both power flow the simultaneously engaging teeth and the largest tooth force are approximately the same**, and the distribution of forces acting to the engaging teeth is also similar.

f) In the case shown in *Figure 11.* the disks of the generator were changed from $d_t = 186{,}3\ mm$ to $d_t = 186{,}1\ mm$ . The radial displacement decreased from $w_0 = 1{,}2\,mm$ to $w_0 = 1{,}1\,mm$ , the semi arc of contact also decreased from $\beta = 34{,}757^o$ to $\beta = 24{,}811^o$ , **the effect to the radius of curvature is negligible**.

g) In the case shown in *Figure 12.* the disks of generators were changed from $d_t = 186{,}3\,mm$ to $d_t = 186{,}1\ mm$ . The radial displacement decreased from $w_0 = 1{,}2\ mm$ to $w_0 = 1{,}2\ mm$ , and the semi arc of contact also decreased from $\beta = 34{,}757^o$ to $\beta = 24{,}811^o$ . Relatively to the variant shown in *Figure 11.* the circular spline was also changed, instead of $x_2 = 4{,}958$ the profile correction factor altered to $x_2 = 5{,}098$ . **The increment in the number of simultaneously engaging teeth is shown by the alteration of the radius of curvature.**

h) In the variant visible on *Figure 12.* the eccentric and the disks were changed, **the arc of contact between the flexspline and the disks was increased** $(2\beta = 85{,}06^o)$ . The radius of curvature of the flexspline, relatively to the previously mentioned cases, was changed slightly in the power flow $2 \to 1$ , and in the power flow $1 \to 2$ **it was changed significantly, due to the influence of the disk to the flexspline**.

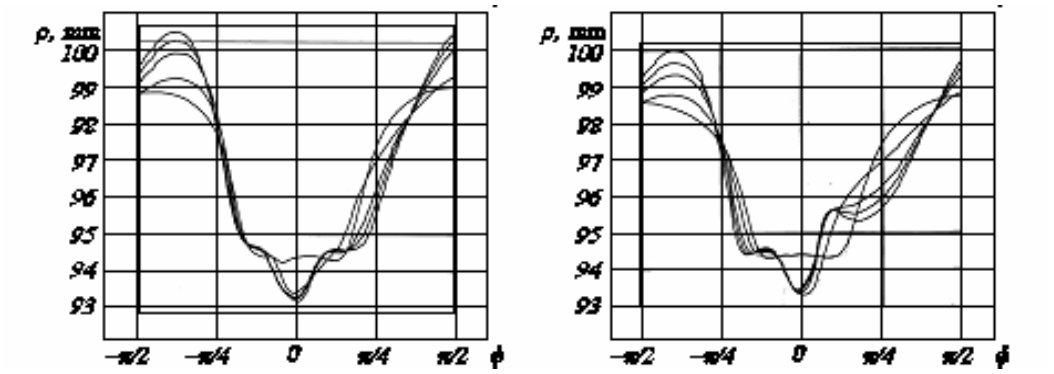
j) In the cases discussed with the help of *Figure 9–12.* it is obvious that **the shape of flexspline diverges depending on the power flow of the drive**.

k) At the power flow of $1 \to 2$ the deflection of flexspline can be limited by increasing the disk diameter.

l) Increasing the normal gap the limitation of deflection of flexspline is reduced.

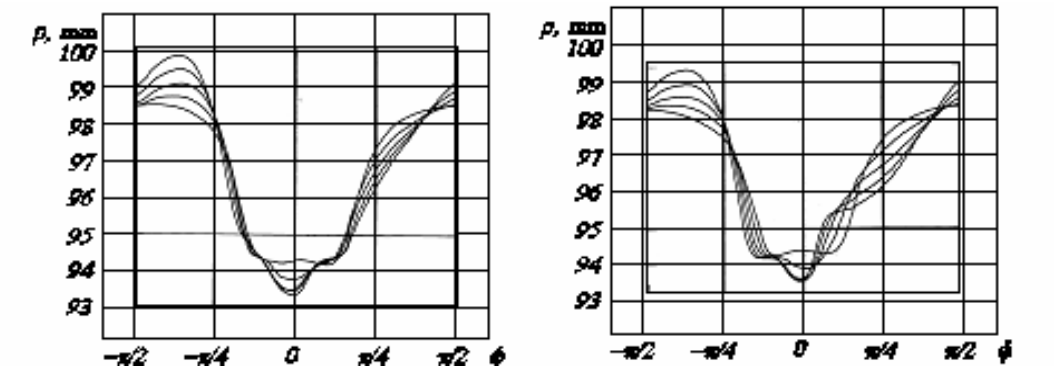
*Gear drive service,* $2 \to 1$ *Gear drive service,* $1 \to 2$

$x_1 = 4{,}555$ , $x_2 = 5{,}098$ , $w_0 = 1{,}2\ mm$ , $e = 3{,}9\ mm$ , $d_t = 186{,}3\ mm$ , $\beta = 34{,}757^o$




*a)* *b)*

$x_1 = 4{,}555$ , $x_2 = 5{,}098$ , $w_0 = 1{,}2\ mm$ , $e = 3{,}9\ mm$ , $d_t = 186{,}1\ mm$ , $\beta = 24{,}811^o$

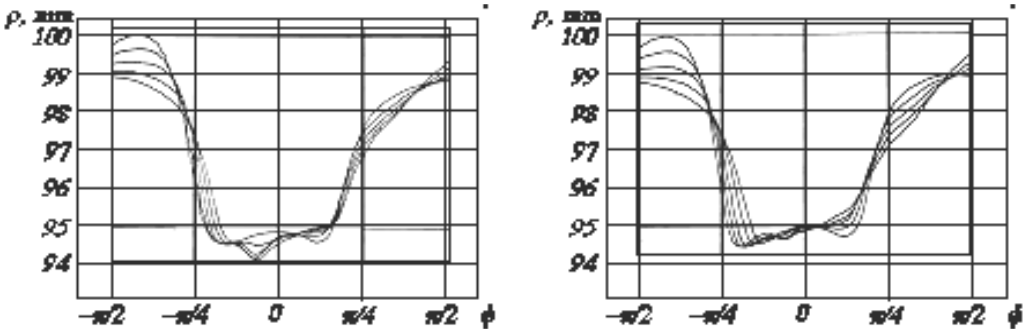



*c)* *d)*

*Figure 12. The radius of curvature, in the function of deviation relatively to the major axis of the generator.*

*Gear drive service,* $2 \to 1$ *Gear drive service,* $1 \to 2$

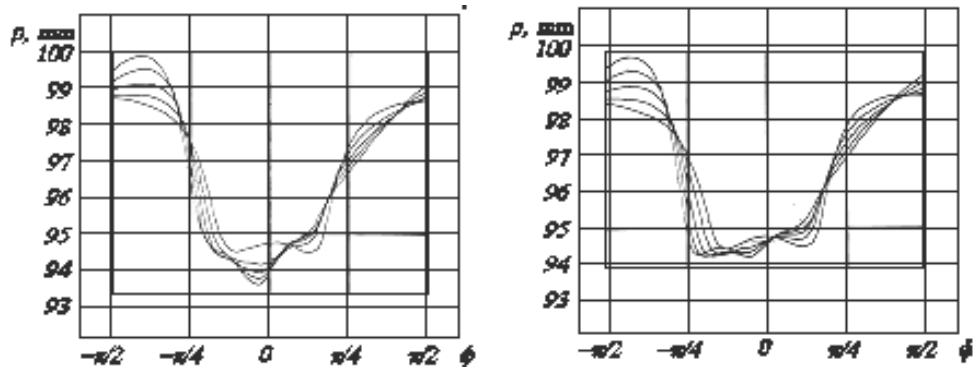
$x_1 = 4{,}555$ , $x_2 = 4{,}958$ , $w_0 = 1{,}2\,mm$ , $e = 3{,}4\,mm$ , $d_t = 186{,}9\,mm$ , $\beta = 42{,}53^o$




*a)* *b)*

$x_1 = 4{,}555$ , $x_2 = 5{,}098$ , $w_0 = 1{,}1mm$ , $e = 3{,}4\,mm$ , $d_t = 186{,}9\,mm$ , $\beta = 42{,}53^o$

*Gear drive service,* $2 \to 1$ *Gear drive service,* $1 \to 2$




*c)* *d)*

*Figure 13. The radius of curvature, in the function of deviation relatively to the major axis*

**10. Summary**

In the present paper the authors examined the relationship among the geometry and load characteristics of a harmonic gear drive containing eccentric disk wave generator. The characteristics were the radial displacement measured next to the back surface of the flexspline, the radius of curvature, the force acting to the tooth of circular spline, the data of geometry and the load of the drive. The conclusions was restricted to the effect of the changed driving elements on the curvature of flexspline.

**Acknowledgement**

"This research was carried out as part of the TAMOP-4.2.1.B-10/2/KONV-2010-0001 project with support by the European Union, co-financed by the European Social Fund."

**REFERENCES**

[1] C. W. Musser: *Elastic-Body Mechanics*. Machine Design, 1961. No. 6. 150–156 p.
[2] J. Péter: *Fogazott hullámhajtómű kapcsolódásának vizsgálata*. (A Miskolci Műszaki Egyetemen elfogadott egyetemi doktori értekezés.) 1981, 174. p.
[3] J. Péter: *Fogaskerék-hullámhajtómű és tengelykapcsoló kapcsolódásának vizsgálata*. (Az MTA Tudományos Minősítő Bizottsága által elfogadott kandidátusi értekezés.) 1992, 111. p.
[4] J. Péter–G. Németh: *A fogaskerék-hullámhajtómű geometriai viszonyai*. Gép, 2005/11–12. 133–137. p.
[5] J. Péter: *A fogaskerék-hullámhajtómű rugalmas alakváltozásának összetevői*. Gép. 2008, 10–11. 111–118. p.
[6] J. Péter–G. Németh: *Rugalmas mechanizmusok*. Gép, 2010/11. 77–82 p.
[7] J. Péter–G. Németh: *Fogaskerék-hullámhajtómű laboratóriumi vizsgálata I.* Gép, 2011.
[8] J. Péter–G. Németh: *Fogaskerék-hullámhajtómű laboratóriumi vizsgálata II.* Gép, 2011.
[9] Sz. A. Suvalov–A. D. Volkov: *Deformacija gibkogo zubcsatogo kolesza dvumja diszkami*. Izv. vuz. Mas. 1971. No 10. 44–49. p.